

Transport through a single-atom junction

This article has been downloaded from IOPscience. Please scroll down to see the full text article.

1998 J. Phys.: Condens. Matter 10 2663

(<http://iopscience.iop.org/0953-8984/10/12/008>)

View [the table of contents for this issue](#), or go to the [journal homepage](#) for more

Download details:

IP Address: 171.66.16.209

The article was downloaded on 14/05/2010 at 16:20

Please note that [terms and conditions apply](#).

Transport through a single-atom junction

José-Luis Mozos^{†§}, C C Wan[†], Gianni Taraschi[†], Jian Wang[‡] and Hong Guo[†]

[†] Centre for the Physics of Materials and Department of Physics, McGill University, Montreal, Quebec, Canada H3A 2T8

[‡] Department of Physics, The University of Hong Kong, Pokfulam Road, Hong Kong

Received 25 September 1997, in final form 8 January 1998

Abstract. We have performed first-principles density functional calculations in conjunction with a three-dimensional evaluation of the quantum scattering matrix for single-atom Si and Al tunnel junctions. We predict the equilibrium conductance and resonance transmission properties. Our results unambiguously show that when the atom is somewhat isolated from the electrodes, the differential electric current should show resonances due to atomic valence orbitals. The conductance resonance peaks may or may not retain a universal value, depending on whether or not there is a partial overlap of the resonance transmissions. Our results also clearly demonstrate the formation of a wire when the atomic junction becomes less and less isolated from the electrodes.

1. Introduction

Using advanced nano-fabrication techniques, it is now possible to fabricate atomic-scale devices whose electronic transport behaviour is completely quantum mechanical. A recent such experiment was reported in reference [1] where electron transport through an isolated Al nanoparticle was investigated. One of the findings was that by measuring the electrical current through this nanometre-sized particle, it is possible to probe its internal discrete electronic states. In the experimental set-up, the nanoparticle was sandwiched by two electrodes and was isolated by tunnelling barriers. On varying a small bias voltage V and measuring the current I , peaks of dI/dV are obtained which indicate the electronic states of the particle. The origin of this resonance behaviour is the matching up of the scattering electron energy with that of the internal electronic states. The observed resonance clustering has been explained by assuming that the steady-state occupation configurations of the electrons are highly nonequilibrium [2]. The idea of isolating a system and studying the resonance transmission has appeared in many different contexts, for example in references [3]. In another important application field, exploiting the band-gap differences of various compound semiconductors such as GaAs and AlGaAs, resonance tunnelling devices have been fabricated and extensively investigated since the original work of Esaki [4]. A tunnelling device may give rise to negative differential resistance due to a quantum resonance, leading to useful electronic applications. The internal electronic states of a nanoparticle come from complicated combinations of atomic and molecular orbitals

[§] Present address: Fritz-Haber-Institut der Max-Planck-Gesellschaft, Faradayweg 4–6, D-14195 Berlin-Dahlem, Germany.

of the atoms forming the particle. In the continuous limit, these states become the size-quantized modes. The nanoparticle of reference [1] involves several thousand atoms; its transport properties are thus quite complicated. On the other hand, the opposite limit of a tunnel junction involving a very small number of atoms is interesting as well, and they are easier to analyse using first-principles *ab initio* methods. The purpose of this work is to report our investigations of the DC conductance of atomic junctions in the limiting case of involving only a single atom, using a first-principles technique by combining the density functional total energy method with the solution of the quantum scattering problem. While this simulates only part of the physics which happens in a nanoparticle, it does capture an essential ingredient of the quantum transport, namely transport through the internal electronic states provided by the atom. We also note that even in the single-atom limit, electrical current which flows through can be experimentally measured, as demonstrated in reference [5].

The theoretical problem of quantum transport through a single atom has recently attracted much attention. Mehrez *et al* have explained the observed features of the electric conduction through an atomic junction on the basis of the behaviour of the density of states [6]. Sautet and Joachim [8] have combined a tight-binding model with the quantum scattering approach to investigate transport through atomic impurities. Yazdani *et al* [5] has investigated off-resonance transmission through a single Xe atom both experimentally and numerically. Lang has studied the behaviour of densities of states of a Mg and a Na atom in between two infinitely large planar electrodes [7] by varying the atom–electrode distance, and confirmed [9] that it is possible to obtain negative differential resistance for atomic contacts, because it could arise as the Fermi energies of two electrodes with narrow densities of states pass each other as the external bias is varied. Finally, the authors have studied the formation of atomic wires and predicted DC as well as AC conductances for these systems [10].

In this work, we provide results on the equilibrium conductance of single-atom junctions for a variety of Si and Al systems. Our results unambiguously show, for a system in the form of an atomic tunnel junction, that when the Fermi energy of the electrodes becomes equal to that of an atomic valence orbital, a resonance peak in the DC conductance is to be expected. This has a manifestation in the differential current dI/dV , in which peaks occur at appropriate voltages due to the quantum resonances mediated by the valence orbital. Hence, by measuring the electrical current through the atomic junction, one can indeed probe the atomic spectra of the single atom. This is consistent with the physical picture of the nanoparticle experiment [1]. Since atomic orbitals have energy spacings in the electron volt range, the quantum resonance will not be smeared out at a room temperature [11]. Furthermore, we found that the usually degenerate atomic orbitals can be split by the presence of electrodes, leading to nearby conductance or differential current peaks. Finally, our results clearly demonstrate how the quasi-1D transport channels become established when the tunnel barriers are reduced, i.e. the change from resonance-like curves to the quantized curve, and thus we observe the crossover from the tunnelling through a single atom to transport through a wire inside which there is an atomic junction. Our results were obtained by combining the pseudopotential-based total energy method with the solution of a 3D quantum scattering problem, and thus were entirely obtained from first-principles techniques.

A particularly interesting question concerns the resonance peak conductance. For a three-dimensional (3D) tunnel junction with symmetric barriers, it can be generally shown [12] that the peak value of the conductance for an isolated singlet resonance is universally $2e^2/h$. On the other hand, reference [7] reported 68% of this value for resonance tunnelling

through the 3s singlet of the Na atom. One reason for this difference could be that the equilibrium Fermi level is close to but not exactly at the 3s state, leading to a slight off-resonance. Nevertheless, it is very interesting to carefully examine the resonances due to atomic levels, especially for cases where there are levels near the equilibrium Fermi energy which are close to each other, and thus the resonances have substantial overlap. For this case the question then arises of whether the peak conductance will retain the universal value. By means of a detailed analysis of Si tunnel junctions, we shall address this question clearly.

In the next section we present the model, the method and the results; the last section is devoted to a discussion and summary.

2. Results

We propose an atomic tunnelling structure as shown schematically in the inset of figure 3—see later. The essential part of the structure consists of two metallic electrodes—they are quantum wires with square-shaped cross-sections, sandwiching a single atom in between. The whole system could in principle be fabricated on top of an insulating substrate by micro-fabricating two electrodes and placing an atom in between using the atomic manipulation ability of STM. To fix the distance between the atom and the electrode, d , vacuum barriers can be established on either side of the atom; thus a double-barrier atomic tunnelling junction is established. We note that there are other methods of establishing barriers, such as using oxidation layers as in the experiment of reference [1], or using appropriate spacer atoms [9]. Here in our model we will simply use vacuum. We emphasize again that although we have concentrated on junctions operating on a single atom, the analysis can certainly be extended to clusters, molecules, or other groups of atoms.

To capture the atomic degrees of freedom, we have combined the *ab initio* pseudo-potential total energy method with a three-dimensional (3D) quantum scattering evaluation of the transmission probabilities [10]. Our numerical procedure consists of essentially two steps. First, we solve for the ground-state properties of the atom and the two electrodes by minimizing the Kohn–Sham total energy functional using a plane-wave basis set. The minimization is achieved using the standard conjugate-gradient technique detailed in the review article [13]. This equilibrium analysis produces the self-consistent effective potential $V_{eff}(\mathbf{r}) \equiv \delta U / \delta \rho(\mathbf{r})$ which is ‘seen’ by all of the electrons including those inside the electrodes. Here $U[\rho]$ is the total self-consistent potential energy while ρ the electron density calculated from the electron wavefunctions. Second, we evaluate the scattering matrix of a particle traversing the system defined by V_{eff} , by solving a 3D scattering problem using an extended transfer-matrix technique. To do this, we divided the entire system (electrodes plus the atomic junction) into many parallel slices along the transport direction (the z -direction); when the division is fine enough, the potential within each slice can be safely approximated as being independent of z . The Schrödinger equation is solved within each slice and the wavefunctions and their derivatives matched at the slice boundaries. In this way a transfer matrix can, in principle, be established which connects the outgoing waves to the incoming waves [14]. The difficulty lies in how to control the numerical stability of the procedure, because there are many evanescent modes which produce exponentially diverging factors. We have solved this problem by finding a method which rearranges the transfer matrix such that these exponentially diverging factors do not appear. This is in a similar spirit to the so-called ‘scattering matrix’ approach [15], but due to some differences in the details of the implementation, our method can be applied in 3D and can compute scattering wavefunctions in addition to the transmission coefficients,

as these are needed [16]. Finally, after obtaining the scattering matrix, we compute the conductance from the Landauer formula [17].

We have focused on junctions made of Si and Al atoms and used the pseudopotentials of references [18, 19] for the core, and the parametrization of reference [20] for the exchange–correlation term. Resonance tunnelling in these systems has not been studied before, although these are the most studied atoms in many other problems. In addition, both atoms have open valence shells and thus we expect the Fermi level of the whole system to be near certain atomic orbitals. The electrodes are modelled by the jellium model where the positive charges are uniformly distributed within the electrodes' volume while electrons are explicitly treated using their wavefunctions. For Si, a jellium has a cross-sectional area of 7.25×7.25 au², a length $L = 30.78$ au, and its charge is specified by the usual parameter $r_s \approx 2.0$ au, mimicking metallic leads. The supercell volume used in our plane-wave *ab initio* calculations is $21.77 \times 21.77 \times 2(L + d)$ au³. For the Al junctions, the lead has a cross-sectional area of 8.79×8.79 au², a length $L = 23.57$ au and a charge density specified by $r_s \approx 2.07$ au. The supercell size for an Al junction is $16.67 \times 16.67 \times 2(L + d)$ au³. The atomic junction set-up with square-shaped leads has a symmetry of space group D_{4h} . We have used an upper energy cut-off of 8 Ryd [21].

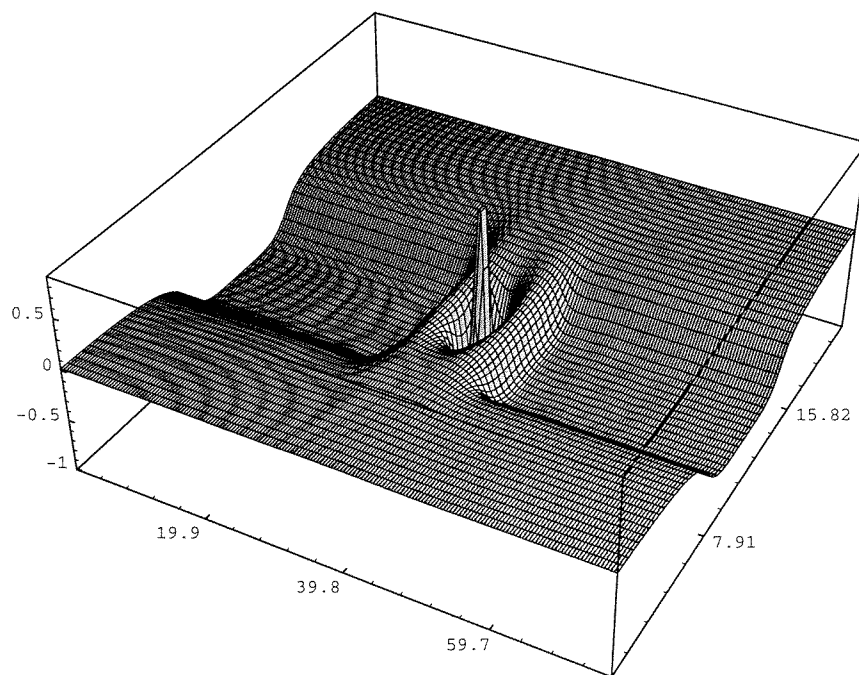


Figure 1. The effective potential V_{eff} for a single-atom Si junction. The atom–lead distance is fixed at $d = 6.9$ au. The vacuum barriers are clearly seen.

For a single adatom on top of a high-density jellium substrate, previous calculations showed [23] that the equilibrium jellium–atom bond length is 2.3 au for Si and 2.6 au for Al [22]. Hence for values of d greater than these values, a vacuum barrier may be established. Figure 1 shows V_{eff} for a Si junction with $d = 6.9$ au. V_{eff} in the 3D leads is essentially a potential well with a depth ~ -0.50 au below the Fermi level of the system. From V_{eff} it

is clear that the atom is quite isolated from the leads by the vacuum barriers. On reducing d to 3.45 and 4.6 au, a lower vacuum barrier is obtained as expected. Similar behaviour is found for Al junctions. In figure 1, the sharp peak at the atomic position reflects the repulsive atomic core, and surrounding the core there is the usual attractive part of the atomic potential.

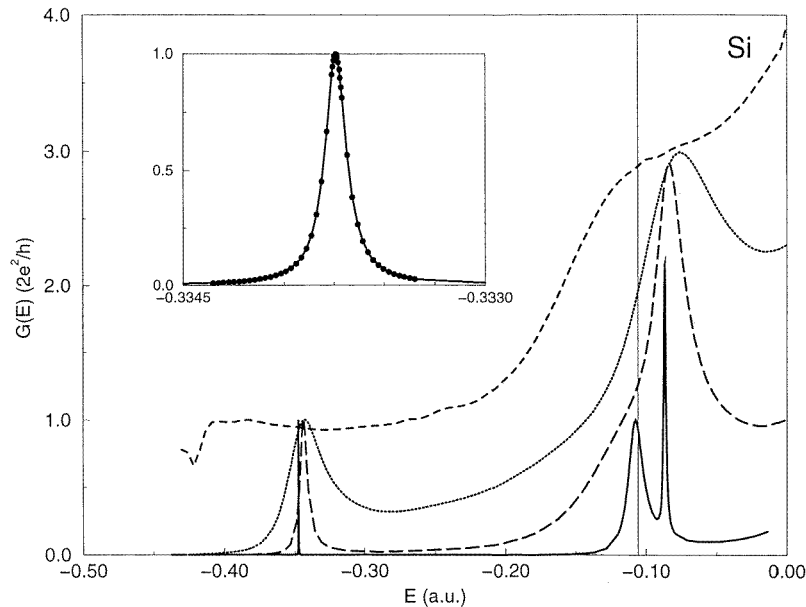


Figure 2. The conductance $G(E)$ as a function of the incoming electron energy E for Si junctions. Dashed line: for $d = 2.3$ au, which is the equilibrium atom–lead distance; dotted line: for $d = 3.45$ au; long-dashed line: for $d = 4.6$ au; solid line: for $d = 6.9$ au. The thin vertical line indicates the calculated equilibrium Fermi level of the system. Inset: resolving the 3s resonance peak for the $d = 6.9$ au case.

Figures 2 and 3 show the conductance G for a number of Si and Al junctions which differ in their jellium–atom junction distances d . When d takes the value of the equilibrium jellium–atom bond length, $G(E)$ shows the expected ‘quantized’ conductance for quasi-1D quantum wires. The quantization plateau is not perfect, because the single-atom junction is too short for establishing perfect quasi-1D transport channels [10]. In addition, the absence of the $G = 2 \times 2e^2/h$ plateau reflects the D_{4h} spatial symmetry of the quantum wire. A striking result, however, is the apparent resonance transmission when the atom is isolated inside a junction by the barriers. For both Si and Al systems, the larger d , the sharper the resonances. This is because a larger d corresponds to a more isolated atom. The resonance peaks must arise from the atomic orbitals since the junction is operating on the electronic structure of the single atom. For a Si atom, the valence configuration is $3s^23p^2$. Thus the equilibrium ‘Fermi’ energy for an isolated atom should be located at the 3p atomic level. For all of the Si junctions, our calculated $E_F \approx -0.10$ au, which is very close to the higher-energy peak position of figure 2. This allows us to identify the resonance peak near -0.09 to -0.10 au as due to the 3p atomic orbital. For the largest d that we studied, i.e. $d = 6.9$ au, the sharp 3p resonance is split into two peaks that are close together as shown in figure 2. We can understand this splitting when we recall that the 3p state is triply

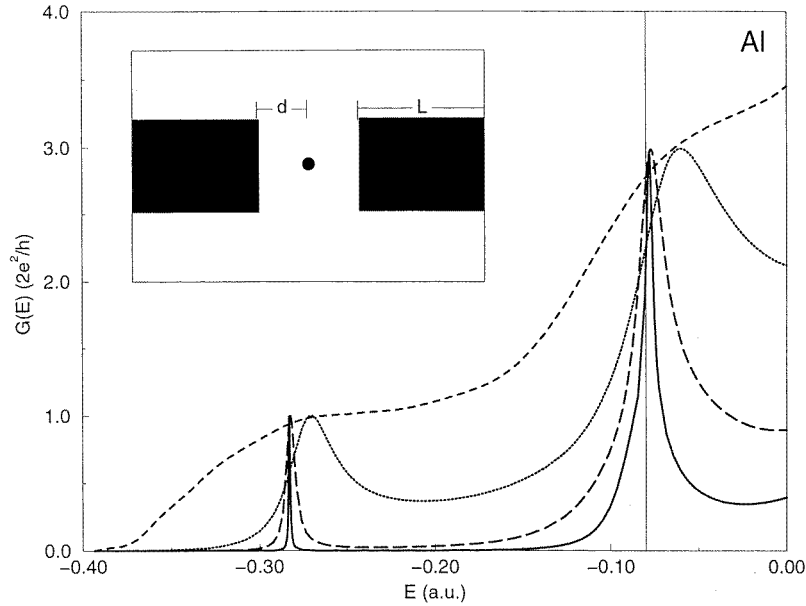


Figure 3. The conductance G for Al junctions. Dashed line: for $d = 2.6$ au; dotted line: for $d = 3.9$ au; long-dashed line: for $d = 5.2$ au; solid line: for $d = 6.5$ au. The thin vertical line indicates the calculated equilibrium Fermi level of the system. Inset: a schematic plot of the atomic junction: an atom is sandwiched between two metallic wires.

degenerate, and its rotational symmetry is broken by the presence of the square-shaped leads which lie along the z -direction. Hence for the single $3p_z$ state, the resonance is marked by $G(E_{3p_z}) \approx 1$ in units of $2e^2/h$. On the other hand, the D_{4h} space group respects the fourfold rotational symmetry in the x - y direction, and thus the degenerate $3p_{x,y}$ states give $G(E_{3p_{x,y}}) \approx 2$. When the lead-atom distance d is smaller, e.g. $d = 3.45$ au or 4.6 au, the atom is not as isolated. For these cases, the resonance width is larger which smears out the $3p$ splits. As a result, the three states of the $3p$ atomic orbital give a $G(E_{3p}) = 3 \times (2e^2/h)$ resonance.

Our results of the $d = 6.9$ au Si junction just presented can answer the question concerning the value of the resonance conductance peak. First, the $3p_z$ peak is slightly higher than 1 while the $3p_{x,y}$ peak is slightly higher than 2, in terms of the conductance quanta. This is due to the partial overlap of these states, as is clearly indicated in figure 2. Hence when there are close resonance states, a partial overlap of DOS can lead to conductance peaks slightly larger than the universal values. Second, while the peak value is larger, the conductance at the Fermi level is sensitive to its position. Figure 2 shows that $G(E_F)$ is very slightly smaller than one quantum for $d = 6.9$ au, and is larger than one quantum for all of the other cases due to the smearing of the $3p$ splittings. For all of the Al junctions investigated, $G(E_F)$ is larger than one quantum, as shown in figure 3.

After understanding the $3p$ resonance peak, it is clear that the lower-energy peak of figure 2 must result from the $3s$ atomic state. Indeed, since $3s$ is a singlet and is far away from other states, we have that $G(E_{3s})$ universally equals $1 \times (2e^2/h)$ independently of the atom-lead distance d as long as a tunnel junction is meaningfully established. For $d = 6.9$ au, the $3s$ peak is extremely sharp; we reproduce it in the inset of figure 2. This result confirms the general result of reference [12] as discussed in the introduction. A

crucial numerical test of these results is based on the distance between the peak positions. For a single Si atom, LDA calculation [24] gives the energy level spacing between the 3s and 3p states as 0.245 au. Our conductance calculation, as shown in figure 2, gives a 3s–3p resonance distance in almost perfect agreement with the LDA spectra, with only small differences due to the level splitting and the presence of the leads. Hence it is unambiguous that the transport in a single-atom junction is mediated by the atomic levels. For Al junctions, as shown in figure 3, all of the results give a physical picture which is consistent with that of the Si system, including the quantitative value of the 3s–3p resonance peak distance. The $3p_z$ split has not occurred in Al junctions because the d -values were not large enough, although we can already observe an indication of it as the $d = 6.5$ au curve shows a slight shoulder near the 3p energy (see figure 3). For different values of d , there is a small but noticeable shift of the relative peak positions (see figures 2 and 3). This is due to the coupling of the atom to the leads, and can be understood on the basis of previous model calculations [25]. Finally, figures 2 and 3 show the formation of a transmissive quantum point contact: on reducing d to the equilibrium bond length between the atom and the leads, the resonance transmission crosses over to the usual quantized conductance with a quasi-1D nature.

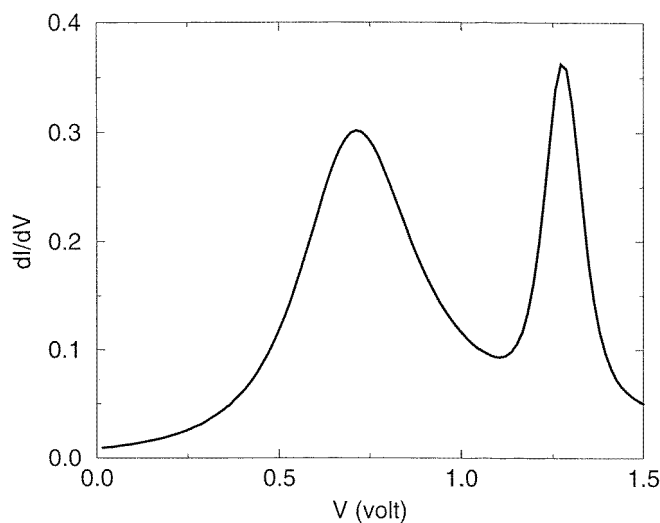


Figure 4. The differential current dI/dV as a function of bias V , for the $d = 6.9$ au Si junction. The double peak reflects the resonance transmission through the 3p states.

Our results for the conductance were presented using the scattering electron energy as the variable. In an experimental measurement, one varies a small bias voltage across the electrodes. The differential current dI/dV shows peaks at certain voltages when a resonance occurs [1]. The equilibrium conductance curves can be converted to obtain an estimate of dI/dV in the standard fashion [26] by integrating the transmission function together with the appropriate Fermi functions of the two electrodes. Figure 4 shows the differential current as a function of the voltage for the Si diode with $d = 6.9$ au at room temperature. The double peak of the differential current reflects the 3p quantum resonances discussed above. We caution that the estimated dI/dV is obtained from equilibrium calculations and thus is only accurate in the small-bias limit. For larger bias, other effects may set in, such as those due to polarization of the charges. The approximate curve of figure 4 does not contain these

physical effects, which could be important.

The results presented in the last section were obtained from first-principles *ab initio* calculations. Beside the resonance conductance peak values which we compared with the discussion of reference [12], certain other features can also be understood analytically. First, using the discussion of reference [12] and Fermi's golden rule, it is not difficult to obtain the resonance width as

$$\Gamma = 2\pi \sum_j |M_j|^2 \delta(E_r - E_j) = \hbar \sum_j w_j$$

where w_j is the rate of tunnelling from the atomic resonance level E_r to the lead level E_j , and M_j is the corresponding tunnelling matrix element connecting E_r to E_j . Since the tunnelling rate decreases exponentially with the barrier size, we expect the resonance widths to do the same, which is clearly seen in our numerical results. Second, we can understand why the $3p_z$ resonance peak width is wider than the $3p_{xy}$ peak. Using a first-order approximation for the tunnelling matrix [27],

$$M_j = \int \chi_j^* V_{\text{lead}} \phi_r \, d^3r$$

where χ_j is the lead state, ϕ_r is the atomic state and V_{lead} is the potential due to the lead. By approximating the lead wavefunctions with finite square-well wavefunctions, and V_{lead} as a potential well, we find $\Gamma_{p_z} / \Gamma_{p_{xy}} = 6.2$ for $d = 6.9$ au. This agrees well with the value of 6.0 obtained from our *ab initio* calculation. We thus conclude that the $3p_z$ resonance peak width is wider than that of the $3p_{x,y}$ peak, because the overlap of the $3p_z$ state with the lead wavefunctions is much larger than the corresponding overlap for the $3p_{xy}$ states.

3. Summary

In summary, we have numerically investigated atomic-scale double-barrier junctions and focused on the equilibrium conductance of these systems. The quantum resonance transmission in this system is through atomic orbitals, and thus the conductances obtained characterize the conduction through a single atom and reveal the valence atomic spectra. The estimated differential current does indeed show peaks, which are the result of resonant transmission through the atomic orbitals. In this work we have focused on two important systems, Si and Al. While their electronic and mechanical properties have been extensively investigated in the literature, here we have, for the first time, studied resonance tunnelling through single-atom junctions made of these atoms. Due to the open valence shell of these atoms, the equilibrium Fermi energy of the system is near some of the atomic orbitals, and thus resonance transmission can be established reasonably easily. The experimental studies of quantum transport through a single atom have been performed using a STM tip, where the single atom is attached, approaching a substrate [5]. In this work we have investigated the tunnelling regime and experimentally this regime can be realized by several ways. A tunnel junction maybe established in the tip-substrate arrangement if 'spacer' atoms are used to separate the STM tip from the absorbed atom through which tunnelling occurs, as suggested by references [9, 3]. The condition for the 'spacers' is that they do not have high densities of states at the equilibrium Fermi energy of the entire junction, thereby providing the necessary tunnel barriers [9]. Another method is to fabricate two electrodes on top of an insulating substrate, as discussed in the introduction, and then use a STM tip to lower an atom to a position in between. Vacuum barriers can thus be established to form a tunnel junction. Finally, for larger junctions, one can simply isolate an atomic-scale particle using insulating materials as shown in the experiment of reference [1]. We emphasize that while

we have concentrated on the model junctions operating on a single atom, for more atoms the physics should still be similar—namely, the differential current should still reflect the internal electronic structure of the system [1]. For more atoms, the resonances would be through the ‘molecular’ orbitals rather than the atomic orbitals identified here.

Acknowledgments

We gratefully acknowledge financial support provided by the NSERC of Canada and FCAR of Quebec. JW is supported by a RGC grant of the Hong Kong Government under grant number HKU 261/95P, and a research grant from the Croucher Foundation. We thank the Computing Centre of the University of Hong Kong for a substantial CPU allocation on their IBM SP2 parallel computer for the numerical analysis presented here.

References

- [1] Ralph D C, Black C T and Tinkham M 1997 *Phys. Rev. Lett.* **78** 4087
- [2] Agam O, Wingreen N S, Altshuler B L, Ralph D C and Tinkham M 1997 *Phys. Rev. Lett.* **78** 1956
- [3] Lyo I W and Avouris Ph 1989 *Science* **245** 1369
Avouris Ph, Lyo I W, Bozso F and Kaxiras E 1990 *J. Vac. Sci. Technol. A* **8** 3405
- [4] Esaki L 1958 *Phys. Rev.* **109** 603
- [5] Yazdani A, Eigler D M and Lang N D 1996 *Science* **272** 1921
- [6] Mehrez H, Ciraci S, Buldum A and Batra I P 1997 *Phys. Rev.* **55** R1981
- [7] Lang N D 1997 *Phys. Rev. B* **55** 4113
- [8] Sautet P and Joachim C 1988 *Phys. Rev. B* **38** 12238
- [9] Lang N D 1997 *Phys. Rev. B* **55** 9364
- [10] Wan C C, Mozos J-L, Taraschi G, Wang Jian and Guo Hong 1997 *Appl. Phys. Lett.* **71** 419
- [11] Pascual J I, Mendez J, Gomez-Herrero J, Baro A M, Garcia N, Landman U, Luedtke W D, Bogachev E N and Cheng H P 1995 *Science* **267** 1793
Snow E S, Park D and Campbell P M 1996 *Appl. Phys. Lett.* **69** 269
- [12] Kalmeyer V and Laughlin R B 1987 *Phys. Rev. B* **35** 9805
- [13] Payne M C, Teter M P, Allan D C, Arias T A and Joannopoulos J D 1992 *Rev. Mod. Phys.* **64** 1045
- [14] Sheng W D and Xia J B 1996 *Phys. Lett.* **220A** 268
- [15] Xu Hongqi 1994 *Phys. Rev. B* **50** 8469
- [16] Due to the complicated nature of the mathematics and algorithm procedures of our extended transfer-matrix technique, we present the details of it elsewhere:
Wan C C, Dejesus T and Guo Hong 1998 *Phys. Rev. B* at press
- [17] Landauer R 1957 *IBM J. Res. Dev.* **1** 233
- [18] Ihm J and Cohen M L 1979 *Solid State Commun.* **29** 711
- [19] Goodwin L, Needs R J and Heine V 1990 *J. Phys.: Condens. Matter* **2** 351
- [20] Goedecker S, Teter M and Hutter J 1996 *Phys. Rev. B* **54** 1703
- [21] We present the results in atomic units: 1 au of energy is 27.2 eV, 1 au of length is 0.529 Å.
- [22] Lang N D 1995 *Phys. Rev. B* **52** 5335
- [23] Lang N D and Williams A R 1978 *Phys. Rev. B* **18** 616
- [24] We obtained the DFT results from the *NIST Basic Reference Data for Electronic Structure Calculations Database* (<http://math.nist.gov/DFTdata/>). We have also independently verified the quoted value.
- [25] Wang Jian, Wang Yongjiang and Guo Hong 1994 *Appl. Phys. Lett.* **65** 1793
- [26] Datta S 1995 *Electronic Transport in Mesoscopic Systems* (New York: Cambridge University Press)
- [27] Chen C J 1993 *Introduction to Scanning Tunneling Microscopy* (New York: Oxford) p 68